A Wideband to Narrowband Tunable Antenna Using A Reconfigurable Filter

Pei-Yuan Qin, Feng Wei, Y. Jay Guo

***Abstract*— A novel microstrip circular disc monopole antenna with a reconfigurable 10 dB impedance bandwidth is proposed in this communication for cognitive radios. The antenna is fed by a microstrip line integrated with a bandpass filter based on a three-line coupled resonator (TLCR). The reconfiguration of the filter enables the monopole antenna to operate at either a wideband state or a narrowband state by using a PIN diode. For the narrowband state, two varactor diodes are employed to change the antenna operating frequency from 3.9 to 4.82 GHz continuously, which is different from previous work using PIN diodes to realize a discrete tuning. Similar radiation patterns with low cross-polarization levels are achieved for the two operating states. Measured results on tuning range, radiation patterns and realized gains are provided, which show good agreement with numerical simulations.**

***Index Terms*—Reconfigurable antenna, cognitive radio, monopole antenna, wideband antenna.**

I. Introduction

Owing to the rapid proliferation of wireless communications systems, the limited electromagnetic spectrum has become more and more congested. On the other hand, it is widely recognized that the current assigned bands are far from being fully utilized. Accordingly, the development of smart communication systems to efficiently use the spectrum resource has attracted significant attention. Cognitive Radio (CR) [1] is regarded as one of the most promising technologies to enhance the spectrum efficiency since it has the capability of learning the channel activities and then deciding on the optimal communication strategies, such as the radiation characteristics, modulation schemes, and network topologies. From a hardware/RF point of view, in order to achieve these flexibilities, an agile RF front-end sub-system composing of reconfigurable antennas [2]-[9] is required.

One of the system strategies made possible by CR is to change the system operating frequency. Specifically, a CR system can sense the spectrum usage and then allocate services to an unoccupied part of the spectrum without causing interference to other users. To this end, it is suggested two separate antennas are required, namely a wideband antenna for scanning the spectrum and a narrowband frequency reconfigurable antenna for communicating.

In the last decades, reconfigurable antennas focusing on narrowband frequency tuning have been extensively investigated [2-5], including dipole antennas, microstrip patch antennas, and *et al*. In order to reduce the size and the complexity of the RF front-end of the cognitive radio system, research activities have been conducted to combine the two desired antennas together by using a single-port fed antenna that can switch between the wideband and narrowband operations. In [10], an ultrawideband (UWB) to three narrowbands microstrip monopole antenna was developed by using reconfigurable impedance matching networks. The narrowband frequency reconfiguration is achieved by using two GaAs field effect transistor (FET) switches to control the connection between different stubs and the main feed line of the monopole. In [11], a Vivaldi antenna capable of switching between a wideband and six discrete narrowbands by inserting two ring slots into the feeding area of the Vivaldi. The two ring slots loaded with fifteen PIN diodes serving as reconfigurable resonators are used to alter the resonant frequencies of the narrowband operation. For the above two novel designs, since the narrowband frequency tuning is realized by using either FET switches or PIN diodes, the number of the switches together with their biasing networks increases with the number of the narrowband states achieved. Although the biasing networks have minimal effects on the antenna radiation characteristics as they are placed away from the radiators, the total cost and the design complexity could increase significantly if a large number of narrowband operations are needed. This may compromise the goal of combining the wideband and reconfigurable narrowband antennas together for the ease of the RF front-end design for CR systems.

In this communication, a new method to design wideband to agile narrowband operations is presented by incorporating a reconfigurable bandpass filter based on a three-line coupled resonator (TLCR) to the feed line of the antenna. The filter can switch between a wide bandpass response and a narrow bandpass response by using a PIN diode, thereby enabling the antenna to operate at either a wideband state or a narrowband state. When the antenna is in the narrowband state, two varactor diodes are employed to enable the reconfiguration of the operating frequency continuously. Since the reconfigurable filter is placed far away from the radiator, its biasing network has very little effect on the radiation characteristics of the antenna. Compared to [10-11], the proposed design can realize a continuous frequency tuning by using only two varactor diodes and one PIN diode, thereby simplifying the biasing network. In addition, better out-of-band rejection is achieved in the proposed design. Measured results show that the wideband state can cover a frequency range from 3.8 GHz to more than 6 GHz, while the narrow band sate can realize a continuous frequency tuning from 3.9 - 4.82 GHz ($|S_{11}|\leq$-10 dB), resulting in a 1.24 tuning ratio.

In Section II, the antenna structure, the operating principle and the biasing network of the proposed configuration are described. Simulation and measurement results of the antenna are provided and compared in Section III. The paper concludes in Section IV.

Manuscript received July 01, 2014. This work was supported by the National Natural Science Foundation of China (NSFC) under Grant 61301071.

P.-Y. Qin and Y. J. Guo are with University of Technology, Sydney, NSW, 2007, Australia. F. Wei is with the Science and Technology on Antenna and Microwave Laboratory, Xidian University, Xi'an, Shaanxi 710071, China. (e-mail: pyqin1983@hotmail.com)

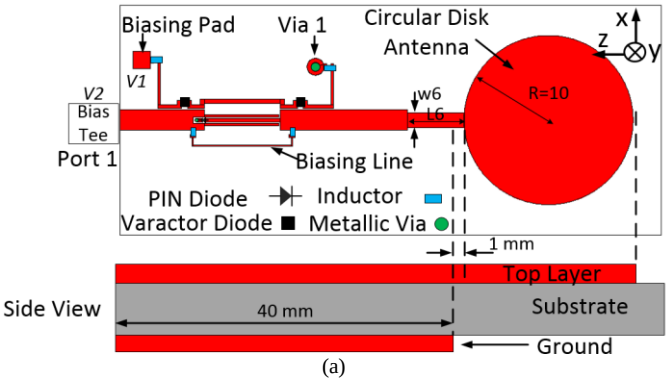

(a)

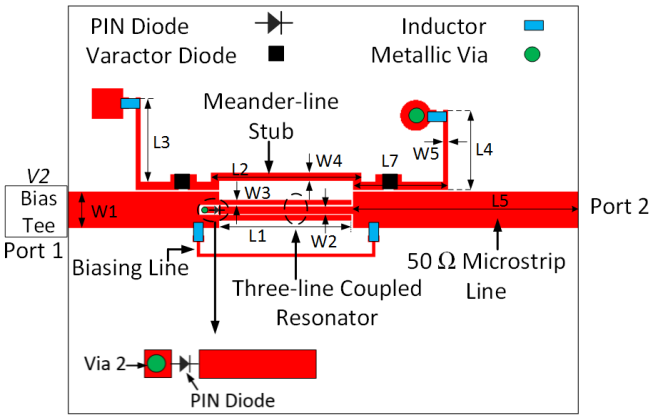

(b)

Fig. 1 Schematics of the proposed antenna: (a) Whole structure; (b) Filter based on a three-line coupled resonator (TLCR).

II. Reconfigurable Antenna Design

Fig. 1 (a) shows the configuration of the reconfigurable monopole antenna. It is printed on the two sides of a 0.787-mm-thick RT/Duroid 5880 substrate (dielectric constant ε_r = 2.2, $tan\delta$ = 0.0009). For the top layer, it is composed of a circular disc as the radiating element and a three-line coupled resonator (TLCR) based bandpass filter integrated with a 50 Ω microstrip feed line. The circular disc monopole antenna with a radius of 10 mm can achieve a very wide 10 dB impedance bandwidth. As seen in the side view of Fig. 1 (a), a ground plane is printed on the bottom layer with a 1 mm gap between the feed point and ground plane. The dimensions of the antenna are given in Table I.

TABLE I Dimensions of the Proposed Antenna (unit: mm)

W1	W2	W3	W4	W5	W6	R
2.4	0.45	0.3	0.5	0.3	1.8	10
L1	L2	L3	L4	L5	L6	L7
8.85	10	5.6	5.3	15	6.8	6.3

Fig. 1 (b) shows the configuration of the filter composing of a TLCR, the input/output 50 Ω microstrip line, a meander-line stub, and the biasing circuits for diodes. By adjusting the impedance of the three high-impedance lines and the distance between them (0.15 mm), a desired bandpass response can be realized [12]. For the middle high impedance line, it is connected to the ground through a PIN diode and a metallic via (via 2). When the diode is switched off, the filter has a wide bandpass performance. In this case, the antenna operates at a wideband state. When the diode is turned on, since the middle high-impedance line is shorted to the ground, the energy coupling between Port 1 and Port 2 is realized mainly through the meander-line stub which is located 0.15 mm above the 50 Ω microstrip lines. In this case, the filter has a narrow bandpass performance and the antenna operates at a narrowband state. Two varactor diodes are inserted into appropriate positions of the stub to vary its electrical length in order to reconfigure the center frequency of the narrowband. In this work, the PIN diode used is MA-COM MA4FCP300 [13]. According to the datasheet, it can be modeled as a 4Ω resistor for the ON state and a parallel circuit consisting of a capacitor of 0.04 pF and a resistor of about 20 kΩ for the OFF state in the simulation using CST Microwave Studio [14]. The GaAs hyperabrupt varactor diodes used are Aeroflex Metellics MGV 125-20-0805 [15], which have a junction capacitance tuning range of 0.1-1pF for a corresponding tuning voltage of 20 to 2 V. A series RLC equivalent circuit used to model the varactor diode in the simulation is shown in Fig. 2. The model includes the diode parasitic inductance and the series resistance, while the total capacitance consists of both parasitic and junction components.

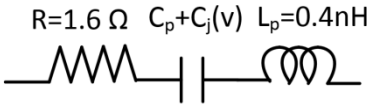

Fig. 2 Equivalent circuit of the varactor diode (C_p = 0.06 pF, C_j = 0.1-1.0 pF)

The performance of the filter (Fig. 1 (b)) has been simulated. Fig. 3 (a) and (b) gives the *S* parameter results for the wideband state and narrowband state, respectively. As seen from the Fig.3, for the wideband state, the insertion loss is less than 0.5 dB. For the narrowband state, when the capacitance of the varactor changes from 1.06 pF to 0.16 pF, the passband of the filter is tuned from 3.85 GHz to 4.76 GHz with the insertion loss varying from 2.8 dB to 1.3 dB. The high insertion loss is mainly attributed to the losses of the varactor diodes which is related to the 1.6 Ω series resistance. A lower insertion loss can be achieved when this resistance is reduced.

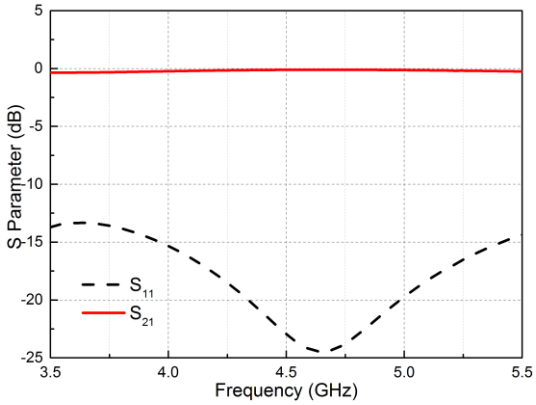

(a)

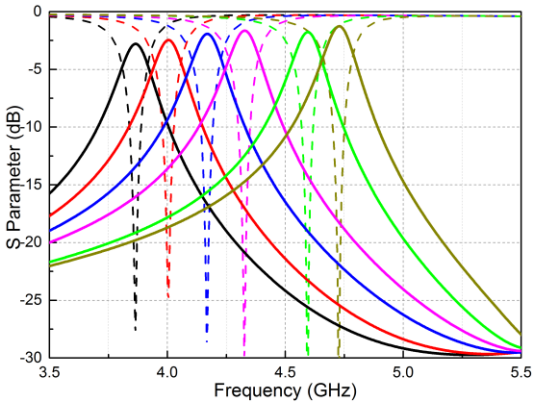

(b)

Fig. 3 Simulated S parameter of the filter: (a) wideband state; (b) narrowband state.

For the biasing of the varactor diodes, one dc biasing voltage labeled as *V1* (Fig. 1 (a)) is connected to the biasing pad. Metalic via 1 is the dc ground for varactor diodes. Two surface-mount inductors from Coilcraft (0402HP, 20 nH) are used to choke the RF signal. Since there are two varactor diodes in series, dc source *V1* should be able to tune from 4 V to 40 V. For the biasing of the PIN diode, another dc biasing voltage labeled as *V2* is used. It is seen from Fig. 1 (b) that one polarity of the PIN diode is connected to the ground through metallic via 2 and another polarity is connected to the middle high impedance line of the TLCR. By using two surface-mount inductors (20 nH) and a biasing line (shown in Fig. 1 (a)), the middle high impedance line is connected with the 50 Ω microstrip line near Port 1 in terms of the DC signal. Therefore, dc source *V2* and the RF signal can be simultaneously fed through a coaxial probe by using a bias tee connected to Port 1. Keithley 2400 SourceMeter is used to provide constant bias current for PIN diodes and variable bias voltages for varactor diodes.

III. Simulated and Measured Results

A. Input Reflection Coefficients

Based on the above analysis, an antenna prototype is fabricated as shown in the inset of Fig. 4 (a). The simulated and measured input reflection coefficients for the wideband state and narrowband state are shown in Fig. 4 (a) and (b), respectively. As mentioned before, when the PIN diode is switched off, the antenna functions as a wideband antenna. Varactor diodes are tuned to be 0.2 pF to produce an acceptable impedance match for this state. It is seen from Fig. 4 (a) that the measured 10 dB impedance bandwidth can cover a frequency band from 3.8 GHz to 6 GHz. When the PIN diode is turned on, the antenna works at the narrowband state. It can be seen from Fig. 4 (b) that the measured operating frequency can be continuously tuned from 3.9 GHz to 4.82 GHz by varying the reversed bias voltage from 4 V to 42 V, corresponding to a 1.24 tuning ratio, while the simulated tuning range is from 3.85 GHz to 4.76 GHz. Reasonably good agreement between the simulated and measured results is obtained, although there are discrepancies in the S_{11} nulls for the wideband state, small frequency shift and deteriorated impedance match for the lower frequency band of the narrowband state compared to the simulated results. The discrepancies can be attributed to the inaccuracies in the fabrication process and variations in the discrete component parameters from the values given in the diode vendor's data sheets. It should be noted that only a few frequency samples are given in Fig. 3 (b) for clarity and readability. If a varactor diode with a wider variation in junction capacitance is used, then the antenna tuning range would be wider. In addition, the out of band rejection for the narrowband operation is very good.

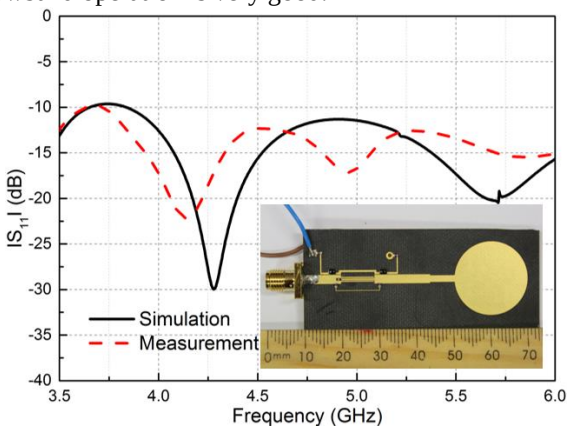

(a)

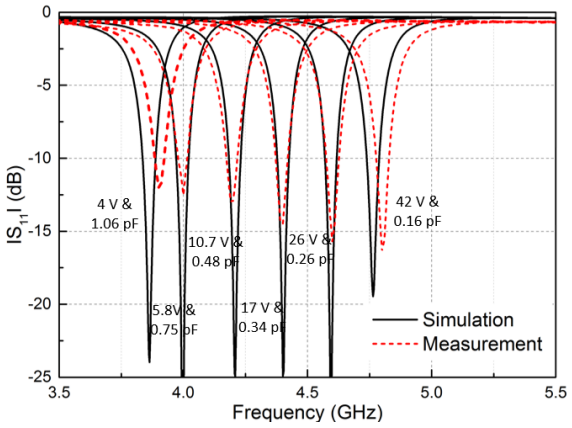

(b)

Fig. 4 Simulated and measured input reflection coefficients of the antenna (a) wideband state; (b) narrowband state.

B. Far-field Radiation Patterns

Far-field radiation patterns were measured for both the wideband and the narrowband states of the antenna using a spherical near-field (SNF) antenna measurement system NSI-700S-50 located at CSIRO, Marsfield, NSW, Australia. A NSI-RF-WR 229 open-ended rectangular waveguide probe was used as the transmitting antenna. The orientation of the rectangular coordinate system in all radiation pattern figures is the same as the one shown in Fig. 1. Simulated and measured normalized radiation patterns are compared at 3.9 GHz and 4.7 GHz for both operating states as shown in Figs. 5 and 6. Good agreement can be found. It can be seen that quasi-doughnut shape patterns and near omni-directional patterns are obtained for the E plane (z-y plane) and H (x-y plane) plane,

respectively. Furthermore, it can be seen that the antenna has similar radiation patterns for different operating states and operating frequencies. The measured maximum cross-polarization levels of E and H planes are about -14 dB and -12 dB, respectively. The simulated cross-polarization for E plane is not shown here as they are very small.

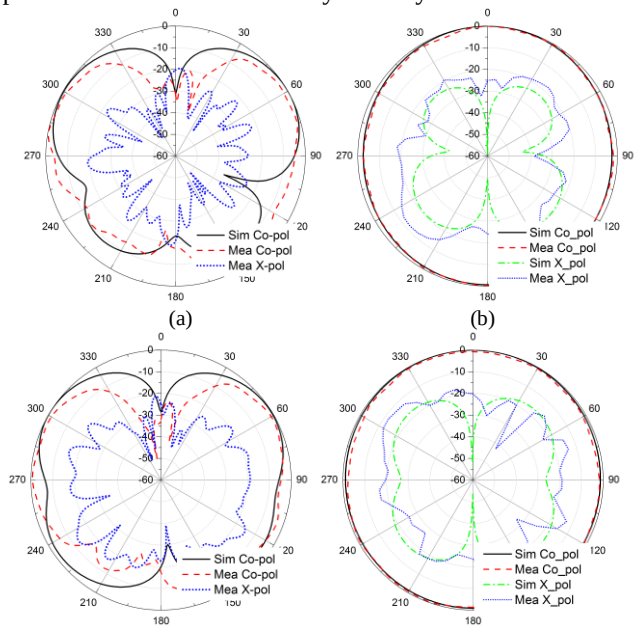

Fig.5 Simulated and measured normalized radiation patterns for wideband state: (a) 3.9 GHz E plane; (b) 3.9 GHz H plane; (c) 4.7 GHz E plane;(d) 4.7 GHz H plane.

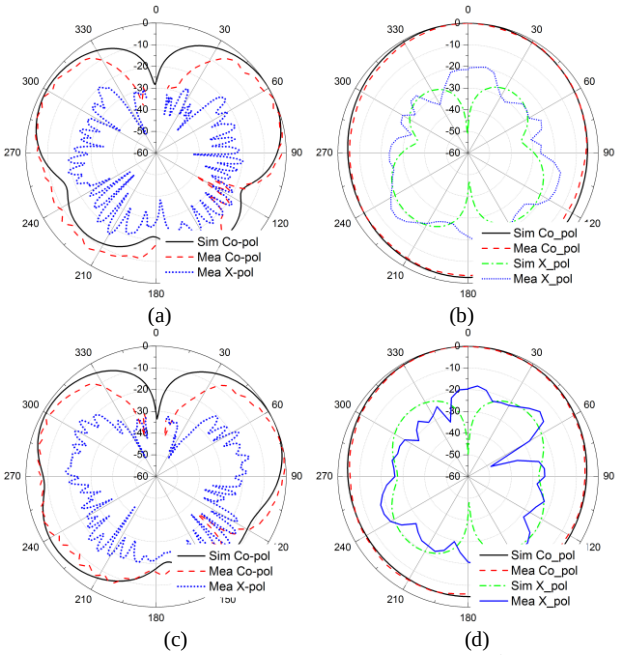

Fig.6 Simulated and measured normalized radiation patterns for narrowband state: (a) 3.9 GHz E plane; (b) 3.9 GHz H plane; (c) 4.7 GHz E plane;(d) 4.7 GHz H plane.

In addition, the simulated and measured realized gains are compared for the two working states of the antenna, which is shown in Fig. 7. For the wideband state, the simulated and measured realized gains are from 3.2 to 4.2 dBi and from 3 to 4.1 dBi, respectively. For the narrowband state, the gains at each frequency point are obtained by tuning the bias voltages of the varactor diodes. The simulated and measured realized gains are from 3.2 to 3.8 dBi and from 2.3-3.8 dBi, respectively. The gain difference between the simulated and measured values at lower frequency band is greater than that of the higher frequency band, which is less than 1 dB and can be due to the same reason that leads to the impedance match discrepancy discussed in the last sub-section. In addition, the measured realized gains of narrowband states 5.8 V (4 GHz), 10.7 V (4.2 GHz), and 17 V (4.4 GHz) versus frequency are given in Fig. 7.

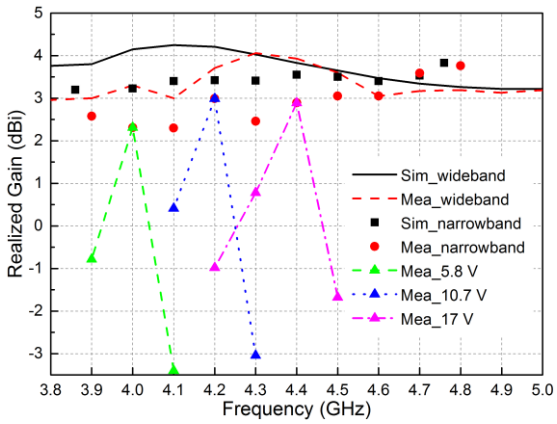

Fig. 7 Simulated and measured realized gains of the antenna.

IV. Conclusion

A reconfigurable wideband to narrowband circular disc antenna has been presented. A PIN diode is used to switch the antenna between the wideband state and the narrowband state, while two varactor diodes are employed to continuously tune the resonant frequency at the narrowband state. Measured results show a continuous tuning from 3.9 to 4.82 GHz for the narrowband state ($|S_{11}|\leq$-10 dB). This makes it suitable for cognitive radio systems. Moreover, since the frequency reconfiguration mechanism proposed is accomplished at the feed line of the antenna without affecting the antenna radiation characteristics, it can be easily applied to other pattern/polarization reconfigurable antennas to realize a combined reconfigurable antenna.

References

[1] J. Mitola and G. Q. Maguire, "Cognitive Radio: making software radios more personal," *IEEE Pers. Commun.*, vol.6, no.4, pp.13-18, Aug. 1999.

[2] S. V. Hum and H. Y. Xiong, "Analysis and Design of a Differentially-Fed Frequency Agile Microstrip Patch Antenna," *IEEE Trans. Antennas Propag.*, vol. 58, no. 10, pp. 3122 - 3130. Oct. 2010.

[3] S. Genovesi, A. D. Candia, and A. Monorchio, "Compact and low profile frequency agile antenna for multistandard wireless communication systems," *IEEE Trans. Antennas Propag*., vol. 62, no. 3, pp. 1019-1026, Mar. 2014.

[4] P.-Y. Qin, A. R. Weily, Y. J. Guo, T. S. Bird, and C. H. Liang, "Frequency reconfigurable quasi-Yagi folded dipole antenna," *IEEE Trans. Antennas Propag*., vol. 58, no. 8, pp. 2742-2747, Aug. 2010.

[5] F. Ghanem, P. S. Hall, and J. R. Kelly, "Two port frequency reconfigurable antenn for cognitive radios," *Electron. Lett.*, vol. 45, no. 11, pp. 534-536, May 2009.

[6] C. G. Christodoulou, Y. Tawk, S. A. Lane, and S. R. Erwin, " Reconfigurable antennas for wireless and space applications," *Proceedings of the IEEE*, vol. 100, no. 7, pp. 2250-2261, Jul. 2012.

[7] Y. Tawk, J. Costantine, and C. G. Christodoulou, " A varactor based reconfigurable filtenna," *IEEE Antennas Wireless Propag. Lett.*, vol. 11, pp. 716–719, 2012.

[8] R. L. Haupt, M. Lanagan, "Reconfigurable antennas," *IEEE Antennas Propag*. Mag., vol. 55, no. 1, pp. 49-61, Feb. 2013.

[9] R. L. Haupt, "Reconfigurable patch with switchable conductive edges," *Microw. Opt. Tech. Lett.*, vol. 51, no. 7, pp. 1757-1760, Jul. 2009.

[10] M. R. Hamid, P. Gardner, P. S. Hall, and F. Ghanem, "Vivaldi antenna with integrated switchable band pass resonator," *IEEE Trans. Antennas Propag*., vol. 59, no. 11, pp. 4008-4015, Nov. 2011.

[11] T. Aboufoul, A. Alomainy, C. Parini, "Reconfiguing UWB monopole antenna for cognitive radio applications using GaAs FET switches," *IEEE Antennas Wireless Propag. Lett.*, vol. 11, pp. 392–394, 2012.

[12] J.-T Guo, E. Shih, "Wideband bandpass filter design with three-line microstrip structures," *IEE Proc. Microw. Antennas Propag.*, vol. 149, no. 5, pp. 243 - 247, Oct. 2002.

[13] M/A-COM Data Sheet for MA4PBL027 beam lead PIN diode.

[14] CST Studio Suit 2012, Computer Simulation Technology. Darmstadt, Germany.

[15] Aeroflex Data Sheet for MGV 125-20-0805-2 varactor diode.